

Brief Reports

Brief Reports are short papers which report on completed research or are addenda to papers previously published in the Physical Review. A Brief Report may be no longer than 3½ printed pages and must be accompanied by an abstract.

Target/projectile mass dependence of light ion yields from heavy ion collisions

R. L. Auble, J. B. Ball, F. E. Bertrand, R. L. Ferguson, I. Y. Lee, R. L. Robinson, and G. R. Young
Oak Ridge National Laboratory, Oak Ridge, Tennessee 37831

(Received 27 March 1987)

Differential cross sections for emission of $Z=1$ and 2 particles are measured for ^{16}O , ^{32}S , and ^{58}Ni projectiles, with energies between 15 and 25 MeV/nucleon, incident on Al, Ti, Ni, Sn, and Au targets. Integral yields are found to have a complex target mass dependence which, for protons, is consistent with model predictions.

Previous studies¹⁻³ have shown that light-ion yields from reactions induced by medium energy projectiles increase monotonically with increasing target mass (A_T). This behavior apparently persists for projectiles with energies as low as 58 MeV/nucleon.³ However, at lower energies the dependence on A_T appears to be quite different. A significant decrease in yield has been reported for heavier targets which, for high energy ejectiles, was attributed to the effect of the Coulomb barrier.⁴ The present study provides additional data on target mass effects for projectiles with energies in the 15- to 25-MeV/nucleon range and examines the influence of projectile mass on the inclusive light ion yields. While the emphasis in this Brief Report is on integral yields, differential cross section data are available upon request.

These measurements were made using beams from the Holifield Heavy Ion Research Facility (HHIRF) coupled accelerators. The projectiles and energies employed were 503.7 MeV ^{32}S , 679.8 MeV ^{32}S , 876.5 MeV ^{58}Ni , and 403.3 MeV ^{16}O . The uncertainty in the beam energy is estimated to be $\pm 0.1\%$. The energy spread in the beam was not determined in the present study but, based on previous experience, is estimated to be about 0.1% full width at half maximum (FWHM). The targets (thickness in mg/cm^2) were ^{27}Al (1.9), ^{46}Ti (5.6), ^{60}Ni (4.1), ^{120}Sn (4.9), ^{124}Sn (3.1), and ^{197}Au (8.3). The target thicknesses were determined by weighing and by energy loss measurements using α particles from a ^{244}Cm source. The uncertainty in the target thickness, based on several determinations, is approximately $\pm 6\%$ for the ^{27}Al , ^{60}Ni , ^{120}Sn , and ^{197}Au targets. The ^{46}Ti and ^{124}Sn targets were found to be nonuniform and the uncertainty for these targets is estimated to be $\pm 15\%$. All target-projectile combinations except $^{16}\text{O} + ^{124}\text{Sn}$ were studied.

The emitted light ions were detected in six, three-element detector telescopes. The first two elements were thin Si ΔE detectors and the third element was a thick

NaI E detector. Detector angles, thicknesses, and solid angles are listed in Table I. The three-element telescopes, with two different amplifier gain settings for the ΔE detectors, were used to cover a wide range of particle energies. The minimum energies which could be detected range from 2.7 MeV for protons to about 10.5 MeV for alphas at $\theta \geq 30^\circ$, and from 5.8 MeV for protons to 21 MeV for alphas at $\theta = 10^\circ$.

The windows on the NaI detectors were $68 \text{ mg}/\text{cm}^2$ aluminum and create a discontinuity in the energy spectra. This gap between the highest energy stopped in the Si detectors and the minimum energy for particles entering the NaI detectors is typically $\sim 2 \text{ MeV}$ wide for protons and $\sim 10 \text{ MeV}$ for ^4He . Particles falling in the gap produce a "punch-through" tail which distorts the low energy part of the spectrum, but most are included in the various particle gates for the purpose of obtaining integral yields.

The Si detectors were calibrated using α particles from a ^{244}Cm source, and the NaI detectors were calibrated by detecting recoil protons from a polyethylene (CH_2) target at scattering angles in the range of 10° – 50° . The uncertainty in the energy calibrations is approximately $\pm 2\%$, except where the energy loss in the detector window is significant.

The uncertainty in the differential cross sections is estimated to be about $\pm 10\%$ for the ^{27}Al , ^{60}Ni , ^{120}Sn , and ^{197}Au targets and about $\pm 17\%$ for the ^{46}Ti and ^{124}Sn targets. These values include an uncertainty of $\pm 3\%$ in the detector solid angles and $\pm 5\%$ in the beam fluence in addition to the uncertainty in the target thickness. Counting statistics become important only at the extreme high energy end of the spectrum.

Proton spectra measured at 10° and 110° from ^{27}Al , ^{60}Ni , and ^{197}Au targets bombarded by 876 MeV ^{58}Ni projectiles are shown in Fig. 1. Spectra from other target-projectile combinations have similar characteris-

TABLE I. Summary of detector parameters.

Angle (deg)	Thickness		E (cm)	Ω (msr)
	ΔE_1 (μm)	ΔE_2 (μm)		
10	250	1000	12.7	0.507
30	75	700	12.7	0.404
50	75	500	12.7	1.82
70	75	500	5.1	2.86
-110	75	500	5.1	5.28
-144	75	500	5.1	5.62

tics, although the peak at forward angles is less pronounced for lighter projectiles. The energy at which the peak occurs in the 10° spectra is nearly independent of the target mass, but the magnitude shows a substantial decrease for the Au target; however, these features are not present in all cases for heavier emitted particles. As

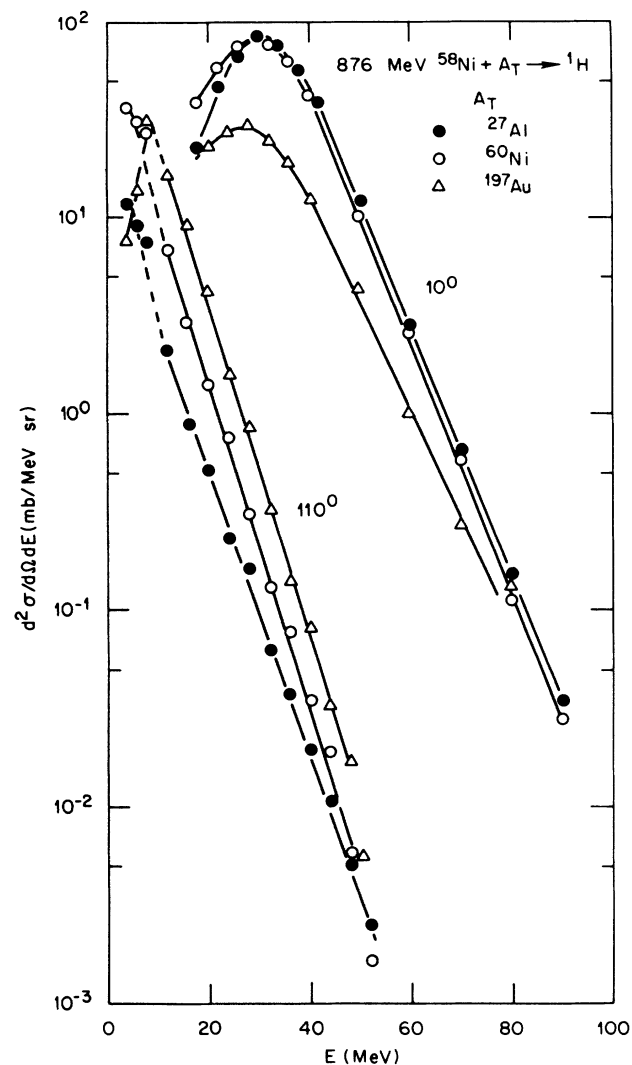


FIG. 1. Proton spectra from 876 MeV ^{58}Ni , on ^{27}Al , ^{60}Ni , and ^{197}Au targets, at detection angles of 10° and 110° . The lines are drawn to guide the eye.

the detection angle increases, the spectra shift to lower energies and become increasingly sensitive to the atomic number of the target nucleus and the emitted particle. The position of the peak in the back-angle spectra, which can be seen in Fig. 1 for the ^{197}Au target, shifts to higher energy with increasing Z of the target or ejectile but is insensitive to the mass and energy of the projectile.

Integral cross sections were determined by summing over all particle energies at each angle after extrapolating the measured spectra to correct for the low energy cutoff and for the "gap" caused by the detector window. The angle integration was performed by assuming an exponential angular dependence between the measured points and extrapolating the angular distributions to 0 and 180° . These approximations will contribute an estimated $\pm 5\text{--}\pm 10\%$ to the uncertainty in the absolute cross sections, but will have little effect on the relative yields. The values thus obtained are listed in Table II and are plotted, as a function of target mass, in Fig. 2.

From Fig. 2 it is apparent that the target mass dependence is very similar for all four projectiles, varying only in magnitude. The deviation from a smooth A_T dependence is obvious for protons, but is only evident with the Au target for composite particles. The large increase in ^3H yields for $A_T > 60$ probably reflects the larger neutron excess of the heavier targets. The proton yields are seen to reach a maximum for $60 < A_T < 120$, in agree-

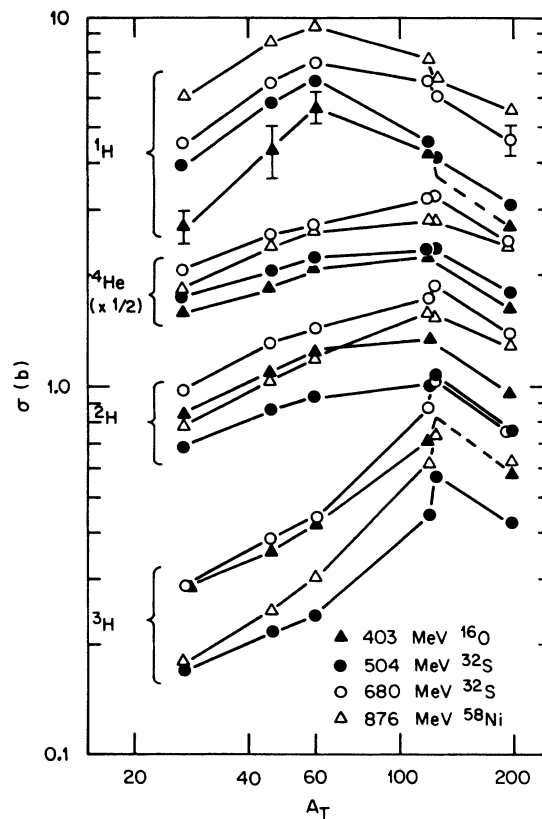


FIG. 2. Integral cross sections for emission of light ions from heavy ion bombardment of various targets. The lines connect data points for a given projectile.

TABLE II. Integral cross sections (b) for $Z=1$ and $Z=2$ particles. Uncertainties are estimated to be $\pm 15\%$ for ^{27}Al , ^{60}Ni , ^{120}Sn , and ^{197}Au , and $\pm 22\%$ for ^{46}Ti and ^{124}Sn targets, except as noted.

Detected	Projectile ^a	Target					
		^{27}Al	^{46}Ti	^{60}Ni	^{120}Sn	^{124}Sn	^{197}Au
^1H	<i>A</i>	2.73	4.41	5.72	4.26		2.67
	<i>B</i>	3.95	5.85	6.74	4.59	4.11	3.11
	<i>C</i>	4.53	6.73	7.50	6.70	6.05	4.61
	<i>D</i>	6.08	8.62	9.46	7.65	6.77	5.61
^2H	<i>A</i>	0.84	1.08	1.23	1.35		0.96
	<i>B</i>	0.69	0.87	0.94	1.00	1.09	0.77
	<i>C</i>	0.99	1.30	1.44	1.74	1.89	1.38
	<i>D</i>	0.78	1.04	1.19	1.58	1.54	1.29
^3H	<i>A</i>	0.29	0.35	0.42	0.71		0.58
	<i>B</i>	0.17	0.21	0.24	0.45	0.58	0.42
	<i>C</i>	0.29	0.39	0.44	0.88	1.08	0.78
	<i>D</i>	0.18	0.25	0.30	0.63	0.75	0.63
$^3\text{He}^b$	<i>A</i>	0.22	0.27	0.29	0.19		0.11
	<i>B</i>	0.15	0.18	0.20	0.12	0.12	0.064
	<i>C</i>	0.25	0.31	0.31	0.24	0.23	0.15
	<i>D</i>	0.15	0.20	0.22	0.20	0.15	0.12
^4He	<i>A</i>	3.20	3.70	4.24	4.56		3.21
	<i>B</i>	3.50	4.13	4.47	4.58	4.60	3.59
	<i>C</i>	4.19	5.16	5.45	6.50	6.60	4.99
	<i>D</i>	3.72	4.80	5.36	5.63	5.71	4.90

^a $A = 403$ MeV ^{16}O ; $B = 504$ MeV ^{32}S ; $C = 680$ MeV ^{32}S ; $D = 876$ MeV ^{58}Ni .

^bNot completely resolved from ^4He . Cross sections should be treated as upper limits.

ment with the results of Awes *et al.*⁴ However, the strong correlation with the incident energy above the barrier reported in Ref. 4, for lower projectile energies, is not observed in the present data. The variation of the proton yields with A_T is consistent with the trends predicted by the precompound emission calculations of Blann⁵ and the direct-plus-evaporation calculations of Friedman.⁶ The latter calculations suggest that most of the target mass dependence is contained in the compound nucleus evaporation component and can be attributed to the higher Coulomb barrier and the lower temperatures reached in the heavier systems. Evaporation calculations for comparison with the proton yields measured here were made using the code PACE2. The pre-

dicted proton emission cross sections for 400 MeV ^{16}O on Al, Ni, Sn, and Au targets are 0.14, 1.29, 3.33, and 0.62 b, respectively. Thus, although the general trend agrees with the data, the maximum yield is predicted to occur at a larger A_T than is observed experimentally. Finally, we note that the composite particle yields are somewhat less sensitive to the mass of the system than are the proton yields which would imply that the compound nucleus evaporation contribution is smaller for these particles.

This research was sponsored by the U.S. Department of Energy under Contract DE-AC05-84OR21400 with Martin Marietta Energy Systems, Inc.

¹S. Nagamiya, M. C. Lemaire, E. Moeller, S. Schnetzer, G. Shapiro, H. Steiner, and I. Tanihata, Phys. Rev. C **24**, 971 (1981).
²R. L. Auble, J. B. Ball, F. E. Bertrand, C. B. Fulmer, D. C. Hensley, I. Y. Lee, R. L. Robinson, P. H. Stelson, C. Y. Wong, D. L. Hendrie, H. D. Holmgren, and J. D. Silk, Phys.

Rev. C **28**, 1552 (1983).

³B. Jakobsson *et al.*, Phys. Lett. **102B**, 121 (1981).

⁴T. C. Awes, S. Saini, G. Poggi, C. K. Gelbke, D. Cha, R. Legrain, and G. D. Westfall, Phys. Rev. C **25**, 2361 (1982).

⁵M. Blann, Phys. Rev. C **23**, 205 (1981); **31**, 1245 (1985).

⁶W. A. Friedman, Phys. Rev. C **29**, 139 (1984).